Smart Structures and Systems, *Vol. 16, No. 5 (2015) 891-918*
DOI: http://dx.doi.org/10.12989/sss.2015.16.5.891

A comprehensive analysis on the discretization method of the equation of motion in piezoelectrically actuated microbeams

M. Zamanian*, M.P. Rezaei, M. Hadilu and S.A.A. Hosseini

Department of mechanical engineering, Faculty of engineering, Kharazmi University, P.O. Box 15719-14911, Tehran, Iran

(Received September 29, 2014, Revised May 18, 2015, Accepted May 31, 2015)

Abstract. In many of microdevices a part of a microbeam is covered by a piezoelectric layer. Depend on the application a DC or AC voltage is applied between upper and lower side of the piezoelectric layer. A common method in many of previous works for evaluating the response of these structures is discretizing by Galerkin method. In these works often single mode shape of a uniform microbeam i.e. the microbeam without piezoelectric layer has been used as comparison function, and so the convergence of the solution has not been verified. In this paper the Galerkin method is used for discretization, and a comprehensive analysis on the convergence of solution of equation that is discretized using this comparison function is studied for both clamped-clamped and clamped-free microbeams. The static and dynamic solution resulted from Galerkin method is compared to the modal expansion solution. In addition the static solution is compared to an exact solution. It is denoted that the required numbers of uniform microbeam mode shapes for convergence of static solution due to DC voltage depends on the position and thickness of deposited piezoelectric layer. It is shown that when the clamped-clamped microbeam is coated symmetrically by piezoelectric layer, then the convergence for static solution may be obtained using only first mode. This result is valid for clamped –free case when it is covered by piezoelectric layer from left clamped side to the right. It is shown that when voltage is AC then the number of required uniform microbeam shape mode for convergence is much more than the number of required mode in modal expansion due to the dynamic effect of piezoelectric layer. This difference increases by increasing the piezoelectric thickness, the closeness of the excitation frequency to natural frequency and decreasing the damping coefficient. This condition is often indefeasible in microresonator system. It is concluded that discreitizing the equation of motion using one mode shape of uniform microbeam as comparison function in many of previous works causes considerable errors.

Keywords: microbeam; piezoelectric actuation; Galerkin method; convergence

1. Introduction

The microelectro-mechanical systems (MEMS) have the low cost, the low power consumption, the high reliability and manufacturability, and the enabling single chip advantages. So, nowadays they are widely being used in high sensitive sensors and actuators (Gopinathan *et al*. 2007). A major material used in these devices is smart piezoelectric material. Piezoelectricity refers to the ability of a material to convert the applied electrical potential into mechanical stress or strain and vice versa.

*Corresponding author, Dr., E-mail: zamanian@khu.ac.ir

Copyright © 2015 Techno-Press, Ltd.
http://www.techno-press.org/?journal=sss&subpage=8 ISSN: 1738-1584 (Print), 1738-1991 (Online)

It is well suited for MEMS, because, piezoelectric materials are able to generate very accurate small motions. Furthermore, one important feature of piezoelectric actuators is high force transition (Simu and Johansson 2002). Often the piezoelectric material is deposited on a part of clamped-clamped or clamped-free microbeam made from Silicon or Silicon Carbide material. Silicon is the preferred material because of its excellent thermal and mechanical properties (small thermal expansion, high melting point, high toughness, and brittleness with no plastic behavior or hysteresis) (Younis 2011). Depending on the application, a DC or AC voltage may be applied between upper and lower sides of piezoelectric layer (Li *et al*. 2006) (Abramovich 1998) (Mahmoodi and Jalili 2007). In microresonator applications with clamped-clamped structure, often, a DC input is used along with a AC input to remove remnant polarization in the piezoelectric material. When piezoelectric layer is powered with a voltage source, an electric field is generated across and perpendicular to the piezoelectric layer. This causes an elongation and strain across the length of the piezoelectric layer. Because it is bonded to the flexible microbeam, the whole structure bends (Younis 2011).

In the literature, Galerkin method has been used to discretize a partial differential equation or to change an ordinary boundary value problem to an algebraic equation. The former change is used when the dynamic solution due to AC actuation is to be evaluated, and the latter is used when the static solution due to DC actuation is to be evaluated. Furthermore, other procedures such as finite element method can be provided to discretize the system (Preidikman *et al*. 2006).Galerkin method considers the differential equation solution as a series of comparison functions which satisfy all the geometric and dynamic boundary conditions of the problem. In the first following paragraph, the important works on piezoelectrically actuated microbeam in which the uniform microbeam mode shapes have been used as comparison functions are presented. In the second paragraph, the works that used the no-uniform microbeam mode shape are introduced. It is noted that when the term "non-uniform microbeam mode shape" is used it means the mode shape of microbeam by considering its discontinuity in the cross section induced by deposited piezoelectric layer.

Mahmoodi and Jalili (2007, 2010) derived the nonlinear equation of motion of piezoelectrically actuated microcantilever under AC actuation with inextensibility assumption. In the discretization of the equations of motion, they used a single mode as comparison function, and solved the resulted initial value problem using the multiple scale perturbation method. The corresponding equation of motion of a piezoelectrically driven microcantilever in the presence of the biological monolayer has been discretized by Mahmoodi *et al*. (2007). The flexural –torsional discretized equation of piezoelectrically actuated microcantilever has been presented by Mahmoodi and Jalili (2008) . The discretized equations by Mahmoodi *et al*. (2007) and Mahmoodi and Jalili (2008) have been solved numerically. Zamanian *et al.* (2008) considered the static deflection of the clamped-clamped microbeam covered by a piezoelectric layer. They used three mode shapes of uniform microbeam as comparison functions when the piezoelectric layer is symmetrically deposited on microbeam. Five mode shapes were used by Raeisi Fard *et al.* (2013) in order to study the static deflection of a microcantilever coated by piezoelectric layer. Shooshtari *et al*. (2012) discretized the motion equation of an AC piezoelectrically actuated viscoelastic microcantilever. Then the discretized equation has been solved by multiple scale perturbation method using a single mode comparison function. Rezazadeh *et al.* (2009) investigated both of clamped-clamped and cantilever microbeam that have on their entire surface a pair of piezoelectric layers under DC voltage. Ghazavi *et al.* (2009) applied Galerkin method to the motion equation of a microcantilever sandwiched at the entire surface with piezoelectric layer under combined AC- DC voltage. The governing equations of piezoelectric laminated free-free or clamped-clamped microbeam that is under the influence of capacitive electrostatic load in one or two opposite directions have been discretized by Azizi *et al.*

(2011, 2013) and Chen *et al.* (2013).

In this paragraph, the works that used the non-uniform microbeam mode shape as comparison function are introduced. Dick *et al.* (2006) approximated the vibration of a clamped-clamped piezoelectrically actuated microresonator considering a single mode. It has been assumed that piezoelectric layer is deposited on the entire length of microbeam. In addition, two electrode patches which cause discontinuity in the microbeam cross section have been assumed to be deposited symmetrically on the left and right side of piezoelectric layer. Bashah *et al*. (2008) analyzed the forced vibration of a flexible Euler-Bernouli beam with step change in the cross section which also occurs in piezoelectricaly actuated microresonators. Korayem and Ghaderi (2013) considered vibration response of a piezoelectrically actuated microcantilever subjected to tip-sample interaction. They separated the equation of motion using a single mode comparison function and then solved it by multiple scale perturbation method.

The literature review shows that when the voltage is AC then a single mode shape of uniform microbeam has been used as comparison function without study about the convergence (Mahmoodi and Jalili 2007,2010) (Shooshtari *et al*. 2012). Although a comparison between theoretical result and experimental result at primary resonance has been presented by Mahmoodi and Jalili (2007) but it has two limitations. The first limitation is the comparison of time histories for a short duration time at the start of vibration, from 0 to 0.1 milisecond, i.e., when it is approximately free vibration. The second limitation is that it was compared for a special sample test, and so different positions of the piezoelectric layer were not studied. In some theoretical works the piezoelectric layer has been assumed to be deposited on the entire length of microbeam i.e. the cross section of microbeam has been considered uniform (Rezazadeh *et al.* 2009) (Ghazavi *et al.* 2009). In some works, the non-uniform microbeam mode shape has been used as comparison function, and so the convergence using uniform microbeam mode shape has not been studied (Dick *et al.* 2006) (Korayem and Ghaderi 2013). Although by Korayem and Ghaderi (2013), the frequency response function, FRF, has been compared to FRF given by uniform microbeam mode shape as comparison function, but it was only using one uniform comparison function. Moreover, the literature review shows that the static deflection due to DC voltage has not been given by the Galerkin method using the non-uniform microbam mode shape as comparison function (Zamanian *et al.* 2008) (Raeisi Fard *et al.* 2013).

It must be noted that since the previous works considered the equation of motion as nonlinear so the convergence was difficult to be studied. So, in this paper the equation of motion is derived with linear assumption. A comprehensive analysis on the convergence of Galerkin method using uniform microbeam mode shape is studied for both clamped–clamped and clamped-free microbeam. The convergence of Galerkin method solution for AC and DC piezoelectric actuation is considered by comparing the results to the results of modal expansion solution. It is noted that since the equation of motion is linear, the modal expansion solution is equivalent to the Galerkin method when non-uniform microbeam mode shape is used as comparison function. The convergence of static solution is verified by comparing the result to the exact solution. The effects of frequency of excitation, coefficient of external damping, location, length and the thickness of piezoelectric layer on convergence are determined. If using one uniform comparison function a good approximation solution obtains for linear equation, then it may be said that the previous nonlinear analysis is also accurate.

2. Modeling and formulation

The system model is a clamped–clamped and clamped-free microbeam which is coated by a

piezoelectric layer as shown in Figs. 1(a) and 1(b). The left and right ends of piezoelectric layer are at distance l_1 and l_2 from the left support of the microbeam, respectively. A DC or AC voltage P as $P_{iC}\cos(\Omega t)$ is applied to piezoelectric layer, whereP_{iC}, Ω and t denote amplitude, frequency and time. When voltage is DC then $P_{iC} = P_{DC}$ and $\Omega = 0$, and when voltage is AC then $P_{iC} = P_{AC}$ and $\Omega \neq 0$.

The Hamilton principle is used to extract the equations of motion, and so the kinetic and potential energies must be constructed. The kinetic energy, *T*, is constructed as

$$T = \frac{1}{2}\int_0^l m(s)\dot{w}^2\, ds \tag{1}$$

where *l* is the length of the microbeam, the dot sign indicates differentiation with respect to time, *t*, and $m(s)$ is mass per unit length, i.e.

$$m(s) = w_b\left(\rho_b t_b + \left(H_{l_1} - H_{l_2}\right)\rho_p t_p\right) \tag{2}$$

where w_b is the width of the microbeam and the piezoelectric layer, $t_b$and t_p are the thickness of the based microbeam and piezoelectric layer, respectively. In addition ρ_b and ρ_p are the mass densities of the based microbeam and the piezoelectric layer, respectively. The expression of H_{l_i} is Heaviside function which is defined according to the longitudinal position as

$$H_{l_i} = Heaviside\ \ function\ (s - l_i) = \begin{cases} 1 & s \geq l_i \\ 0 & s < l_i \end{cases} \quad i = 1,2\ . \tag{3}$$

The piezoelectric layer is not attached to the entire length of the microbeam. In the part where there is no piezoelectric layer, the neutral axis is the midline of the microbeam cross section. In the part where the piezoelectric layer is attached, the neutral axis is at distance $\bar{z}_n$ from the midline of based microbeam cross section as follow

$$\bar{z}_n = \frac{E_p t_p (t_p + t_b)}{2(E_b t_b + E_p t_p)} \tag{4}$$

where E_b and E_p are the elasticity modulus of the microbeam and the piezoelectric layer, respectively. Here, the electrical displacement is one dimensional; therefore, the relation between stress and strain for the microbeam and piezoelectric layer may be constructed as follows (Mahmoodi *et al*. 2007)

$$\sigma_p = E_p\varepsilon - E_p d_{31}\frac{P}{t_p}\ , \qquad \sigma_b = E_b\varepsilon \tag{5}$$

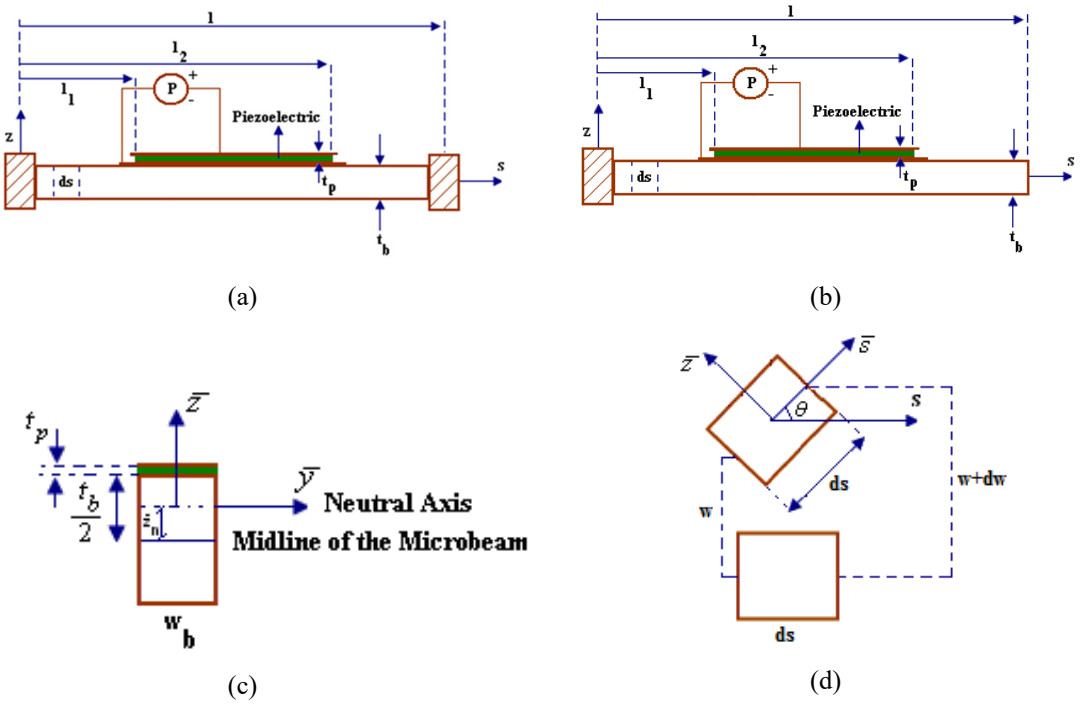

Fig. 1 (a) clamped-clamped model, (b) cantilever model, (c) the system cross section when $l_1 \le s \le l_2$, (d) free body diagram of a deflected element of microbeam

where σ_p and σ_b are the axial stresses of the piezoelectric layer and the microbeam, respectively. Moreover d_{31} is the transversal piezoelectric strain coefficient, and ε is the strain in the cross section of the system. Here it is assumed that the microbeam is subjected to pure bending, and so the strain may be written as follow (Hagedorn and DasGupta 2007)

$\varepsilon = -\kappa \bar{z}$

where κ is the curvature bending of the microbeam in the *sz*-plane, which is obtained as follows

$$\kappa = \left|\frac{d\vec{T}}{ds}\right| = \left|\frac{d\left(\cos\theta \times \vec{i} + \sin\theta \times \vec{j}\right)}{ds}\right| = \left|-\theta' \sin\theta \times \vec{i} + \theta' \cos\theta \times \vec{j}\right| = \theta' \tag{7}$$

where $\vec{T}$ is the unit vector that shows the direction of deflected element, and θ is the angle of element with respect to horizontal direction shown in Fig. 1(d). According to Fig. 1(d)

$$\sin\theta = \frac{dw}{ds} = w' \ , \ \cos\theta = 1 \ \Rightarrow \ \tan\theta = w' \Rightarrow \theta = \tan^{-1} w' \tag{8}$$

where the over prime denotes the derivative with respect to s in all the equations. By employing

the Taylor series expansion of θ and dropping the nonlinear term, Eq. (7) yields

$$\kappa = w'' \ . \tag{9}$$

The strain potential energy of the system, V, may be obtained as follows

$$V = \int_{V_b} \int_0^{\varepsilon} \sigma_b d\varepsilon dV_b + \int_{V_p} \int_0^{\varepsilon} \sigma_p d\varepsilon dV_p$$

$$= \int_0^l \int_{-\frac{t_b}{2}}^{\frac{t_b}{2}} \int_0^{\varepsilon} \left(1 - H_{l_1}\right) \sigma_b w_b d\varepsilon d\bar{z} ds + \int_0^l \int_{-\frac{t_b}{2}-\bar{z}_n}^{\frac{t_b}{2}-\bar{z}_n} \int_0^{\varepsilon} \left(H_{l_1} - H_{l_2}\right) \sigma_b w_b d\varepsilon d\bar{z} ds$$

$$+ \int_0^l \int_{\frac{t_b}{2}-\bar{z}_n}^{\frac{t_b}{2}-\bar{z}_n+t_p} \int_0^{\varepsilon} \left(H_{l_1} - H_{l_2}\right) \sigma_p w_b d\varepsilon d\bar{z} ds + \int_0^l \int_{-\frac{t_b}{2}}^{\frac{t_b}{2}} \int_0^{\varepsilon} H_{l_2} \sigma_b w_b d\varepsilon d\bar{z} ds \tag{10}$$

where dV_b and dV_p show the volume differential element of the microbeam and the piezoelectric layer, respectively. To simplify Eq. (10), first, one must substitute Eqs. (5) and (6) into Eq. (10) and then integrate the resulting expression. In final one obtains

$$V = \frac{1}{2} \int_0^l C_\eta(s) \kappa^2 ds + \int_0^l C_\gamma(s) P \kappa ds \tag{11}$$

where

$$C_\eta(s) = \left(1 - H_{l_1}\right) E_b I_b + \left(H_{l1} - H_{l_2}\right) E_b \bar{I}_b + \left(H_{l1} - H_{l_2}\right) E_p I_p + H_{l_2} E_b I_b \ ,$$

$$C_\gamma(s) = \left(H_{l_1} - H_{l_2}\right) \frac{E_p d_{31} \bar{A}_p}{t_p} \ ,$$

$$I_b = \frac{w_b t_b^{\,3}}{12} \ ,$$

$$\bar{I}_b = \frac{w_b t_b^{\,3}}{12} + t_b w_b \bar{z}_n^{\,2} \ ,$$

$$\bar{A}_p = \frac{w_b}{2}\left(t_b t_p + t_p^2 - 2 t_p \bar{z}_n\right) \ ,$$

$$I_p = w_b\left(\overline{z}_n{}^2 t_p - \left(t_p t_b + t_p{}^2\right)\overline{z}_n + \frac{1}{3}\left(t_p{}^3 + \frac{3}{4}t_b{}^2 t_p + \frac{3}{2}t_p{}^2 t_b\right)\right). \tag{12}$$

Applying the Hamilton principle

$$\int_{t_1}^{t_2}\left(\delta\left(T - V\right) + \delta W_F\right)dt = 0 \tag{13}$$

In the above, δW_F is the virtual work related to damping force as

$$\delta W_F = c_E \dot{w}\,\delta w \tag{14}$$

where c_E is the coefficient of external viscous damping. Differential equation of motion for both the clamped-clamped and cantilever microbeam in the transverse direction is given as follows

$$m(s)\ddot{w} + c_E\dot{w} + \left(C_\eta(s)w''\right)'' + P\left(C_\gamma(s)\right)'' = 0\,. \tag{15}$$

In addition, the associated boundary conditions for clamped-clamped microbeam are and for clamped-free are

$$w\big|_{s=0} = 0, \quad w'\big|_{s=0} = 0, \quad w\big|_{s=l} = 0, \quad w'\big|_{s=l} = 0 \tag{16}$$

and for clamped-free are

$$w\big|_{s=0} = 0, \quad w'\big|_{s=0} = 0, \quad w''\big|_{s=l} = 0, \quad w'''\big|_{s=l} = 0\,. \tag{17}$$

To transform the equation into a dimensionless form, the following new variables are introduced

$$v = -\frac{w}{t_b}\,, \quad x = \frac{s}{l}\,, \quad \tau = \frac{t}{T}\,, \quad T = \sqrt{\frac{\rho_b w_b t_b l^4}{E_b I_b}}\,. \tag{18}$$

So, the dimensionless form of Eq. (15) will be

$$m(x)\frac{\partial^2 v}{\partial\tau^2} + c\frac{\partial v}{\partial\tau} + \frac{\partial^2}{\partial x^2}\left(H(x)\frac{\partial^2 v}{\partial x^2}\right) - \alpha P\frac{d^2}{dx^2}\left(H_{l_1/l} - H_{l_2/l}\right) = 0 \tag{19}$$

where

$$m(x) = 1 + \left(H_{l_1/l} - H_{l_2/l}\right)\frac{\rho_p t_p}{\rho_b t_b}\,,$$

$$H(x) = \left(1 - H_{l_1/l}\right) + \frac{\bar{I}_b}{I_b}\left(H_{l_1/l} - H_{l_2/l}\right) + \frac{E_p I_p}{E_b I_b}\left(H_{l_1/l} - H_{l_2/l}\right) + H_{l_2/l}\,,$$

$$\alpha = \frac{E_p d_{31} \bar{A}_p l^2}{E_b I_b t_p t_b} \ ,$$

$$c = c_E \sqrt{\left(\frac{l^4}{\rho_b w_b t_b E_b I_b} \right)} \ . \tag{20}$$

It is noted that αP is dimensionless measure for the bending moment due to the piezoelectric effect. Moreover, the associated boundary conditions in non-dimension form for Clamped-clamped microbeam are

$$v\big|_{x=0} = 0, \quad \left.\frac{\partial v}{\partial x}\right|_{x=0} = 0, \quad v\big|_{x=1} = 0, \quad \left.\frac{\partial v}{\partial x}\right|_{x=1} = 0 \tag{21}$$

and for cantilever microbeam is

$$v\big|_{x=0} = 0, \quad \left.\frac{\partial v}{\partial x}\right|_{x=0} = 0, \quad \left.\frac{\partial^2 v}{\partial x^2}\right|_{x=1} = 0, \quad \left.\frac{\partial^3 v}{\partial x^3}\right|_{x=1} = 0 \ . \tag{22}$$

It is noted that the equations of motion are derived without considering any axial loads. Hence it is assumed that the structure does not experience buckling, due to the absence of axial forces. However, in practice, a constant axial force may be produced along the length of clamped-clamped microbeam due to the residual stress during manufacturing process (Dick *et al.* 2006). Therefor in this situation, the system may be under buckling due to this axial load (Li and Balachandran 2006).

3. Exact static deflection

By setting the differentiation of displacement with respect to time equal to zero in Eq. (19) and by setting $\mathrm{P_{iC}} = \mathrm{P_{DC}}, \Omega = 0$, the differential equation of static deflection $\mathrm{v_s}$ will be

$$\frac{d^2}{dx^2}\left(H(x) \frac{d^2 v_s}{dx^2} \right) - \alpha P_{DC} \frac{d^2}{dx^2}\left(H_{l_1/l} - H_{l_2/l} \right) = 0 \ . \tag{23}$$

Now, Eq. (23) is integrated two times, so

$$H(x) \frac{d^2 v_s}{dx^2} - \alpha P_{DC} \left(H_{l_1/l} - H_{l_2/l} \right) = C_1 x + C_2 \tag{24}$$

where C_1 and C_2 are the constants of integrating. To solve the above equation v_s is considered as fallow

$$v_s = \left(1 - H_{l_1/l} \right) v_{s_1} + \left(H_{l_1/l} - H_{l_2/l} \right) v_{s_2} + \left(H_{l_2/l} \right) v_{s_3} \tag{25}$$

where v_{s_1}, v_{s_2} and v_{s_3} are the static deflection of microbeam at the part of $[0 \quad l_1/l)$, $(l_1/l \quad l_2/l)$ and $(l_2/l \quad l]$, respectively. Substituting Eq. (25) into Eq. (24), the associated differential equation to any part of the microbeam achieves. So the differential equation at the first part, i.e., $[0 \quad l_1/l)$ becomes

$$\frac{d^2 v_{s_1}}{dx^2} = C_1 x + C_2 \quad \Rightarrow \quad v_{s_1} = \frac{1}{6}\mathrm{C_1 x^3} + \frac{1}{2}\mathrm{C_2 x^2} + \mathrm{C_3 x} + \mathrm{C_4} \ . \tag{26}$$

For the second part, i.e. $(l_1/l \quad l_2/l)$ one obtains

$$\left(\frac{\bar{I}_b}{I_b} + \frac{E_p I_p}{E_b I_b}\right)\frac{d^2 v_{s_2}}{dx^2} = C_1 x + C_2 + \alpha P_{DC}$$
$$\Rightarrow v_{s_2} = \frac{1}{\left(\dfrac{\bar{I}_b}{I_b} + \dfrac{E_p I_p}{E_b I_b}\right)}\left(\frac{1}{6}\mathrm{C_1 x^3} + \frac{1}{2}\left(\mathrm{C_2} + \alpha P_{DC}\right)\mathrm{x^2} + \mathrm{C_5 x} + \mathrm{C_6}\right) \tag{27}$$

and the differential equation governed on the last part, i.e., $(l_2/l \quad l]$ becomes

$$\frac{d^2 v_{s_3}}{dx^2} = C_1 x + C_2 \quad \Rightarrow \quad v_{s_3} = \frac{1}{6}\mathrm{C_1 x^3} + \frac{1}{2}\mathrm{C_2 x^2} + \mathrm{C_7 x} + \mathrm{C_8} \tag{28}$$

where $C_i, i = 3..8$ are unknown coefficients. The boundary conditions for clamped-clamped and clamped-free microbeam is identical to Eqs. (21) and (22), respectively. The only difference is that here v must be replaced by $\mathrm{v_{s_1}}$ in x=0 and by v_{s_3} in x=1. By substituting the boundary conditions and the following continuity conditions into Eqs. (26) and (27) a system of algebraic equations is obtained.

$$v_{s_1}\Big|_{x=l_1/l} = v_{s_2}\Big|_{x=l_1/l}, \qquad \frac{\partial v_{s_1}}{\partial x}\Big|_{x=l_1/l} = \frac{\partial v_{s_2}}{\partial x}\Big|_{x=l_1/l},$$
$$v_{s_2}\Big|_{x=l_2/l} = v_{s_3}\Big|_{x=l_2/l}, \qquad \frac{\partial v_{s_2}}{\partial x}\Big|_{x=l_2/l} = \frac{\partial v_{s_3}}{\partial x}\Big|_{x=l_2/l} \ . \tag{29}$$

Solving the outcome equations, the coefficients $C_i, i = 1..8$ are given. By substituting the coefficients of $C_i, i = 1..8$ into Eqs. (26)-(28) and then applying Eq. (25), an exact solution is found for static deflection.

4. Galerkin method solution

In Galerkin method the solution of Eq. (19) can be expressed as

$$v(x,\tau)=\sum_{i=1}^{M} a_i(\tau)\Phi_i(x) \tag{30}$$

where $\Phi_i(x)$ is the ith comparison function which should satisfy all dynamic and geometry boundary conditions, M represents the number of comparison functions, and $a_i(\tau)$ is the corresponding unknown generalized coordinate. It is noted that in this section, the mode shape of uniform microbeam is used as comparison function. By substituting Eq. (30) into Eq. (19), multiplying the outcome by $\Phi_j(x)$, and integrating the results from x=0 to x=1, a set of coupled ordinary-differential equations are derived as

$$\begin{aligned} eq_j = \sum_{i=1}^{M}\Bigg[& \frac{d^2 a_i(\tau)}{d\tau^2}\int_0^1 m(x)\Phi_j(x)\Phi_i(x)dx \\ & + c\frac{da_i(\tau)}{d\tau}\int_0^1 \Phi_j(x)\Phi_i(x)dx \\ & + a_i(\tau)\int_0^1 \Phi_j(x)\frac{d^2}{dx^2}\left(H(x)\frac{d^2\Phi_i(x)}{dx^2}\right)dx\Bigg] \\ & - \alpha P_{AC}\int_0^1 \Phi_j(x)\frac{d^2}{dx^2}\left(H_{l_1/l} - H_{l_2/l}\right)dx = 0 . \end{aligned} \tag{31}$$

Derivative of Heaviside function in the integration causes an enormous calculation error in mathematical application. Therefore the derivative of Heaviside function is eliminated using the integration by part. It is noted that for an arbitrary continuous function f(x) one can write

$$\int f(x)\frac{d^2}{dx^2}\left(Heaveside(x-a)\right)dx = -\left.\frac{df}{dx}\right|_{x=a} \tag{32}$$

where a is a point between the domain of [0..l]. Integrating by parts from Eq. (31), in addition, by considering the orthogonally conditions for comparison functions, here uniform microbeam mode shape, and applying the boundary conditions, the process is completed as

$$\begin{aligned} eq_j = \sum_{i=1}^{M}\Bigg[& \frac{d^2 a_i(\tau)}{d\tau^2}\int_0^1 m(x)\Phi_j(x)\Phi_i(x)dx\Bigg] \\ & + c\frac{da_j(\tau)}{d\tau} \\ & + \sum_{i=1}^{M}\Bigg[a_i(\tau)\int_0^1 \frac{d^2\Phi_j(x)}{dx^2}H(x)\frac{d^2\Phi_i(x)}{dx^2}dx\Bigg] \\ & + \alpha P_{AC}\left(\left.\frac{d\Phi_j}{dx}\right|_{l_1/l} - \left.\frac{d\Phi_j}{dx}\right|_{l_2/l}\right) = 0 . \end{aligned} \tag{33}$$

Solving set of above differential equations, the generalized coordinate $a_i(\tau)$ are obtained. By substitution $a_i(\tau)$ into Eq. (30) the approximate solution of Eq. (19) is obtained.

If one set $\Omega = 0, P = P_{DC}$, and let the terms including derivative with respect to time, τ , to be

equal to zero in Eq. (33) then the static solution would be obtained. It is noted that by these assumptions, the generalized coordinate $a_i(\tau)$ will be as an algebraic coefficient a_i independent of time.

Here the uniform microbeam mode shapes are considered as comparison function. The mode shape of a clamped-clamped and cantilever uniform microbeam is

$$\Phi_i = C_{1i}\cosh(\beta_i x) + C_{2i}\sinh(\beta_i x) + C_{3i}\cos(\beta_i x) + C_{4i}\sin(\beta_i x)\ , \quad i = 1..M\ . \tag{34}$$

By applying the boundary conditions of microbeams the associated constant coefficients are obtained. In Eq. (34) β_i are related to natural frequencies and can be calculated from the following equations

$$\cos(\beta_i)\cosh(\beta_i) - 1 = 0$$
$$1 + \cos(\beta_i)\cosh(\beta_i) = 0 \tag{35}$$

where the former equation is for clamped-clamped microbeam and the latter is for microcantilever microbeam.

5. Modal expansion solution

In this method the solution is expanded as series (30). The only difference is that $\Phi_i(x)$ is the exact mode shape of system. The mode shapes of the microbeam considering the geometric effect of piezoelectric layer are achieved by solving the homogenous part of Eq. (19). Since the microbeam is divided into three segment, the mode shapes of systems are achieved as follow

$$\Phi_i(x) = \left(1 - H_{l_1/l}\right)W_{1i}(x) + \left(H_{l_1/l} - H_{l_2/l}\right)W_{2i}(x) + H_{l_2/l}W_{3i}(x)\ . \tag{36}$$

And

$$\begin{cases} W_1(x) = C_1\cosh(\beta_1 x) + C_2\sinh(\beta_1 x) + C_3\cos(\beta_1 x) + C_4\sin(\beta_1 x) \\ W_2(x) = C_5\cosh(\beta_2 x) + C_6\sinh(\beta_2 x) + C_7\cos(\beta_2 x) + C_8\sin(\beta_2 x) \\ W_3(x) = C_9\cosh(\beta_3 x) + C_{10}\sinh(\beta_3 x) + C_{11}\cos(\beta_3 x) + C_{12}\sin(\beta_3 x) \end{cases} \tag{37}$$

where

$$\beta_{1i} = \beta_{3i} = \sqrt{\omega_i} \quad , \quad \beta_{2i} = \left(\frac{1 + \left(\frac{\rho_p t_p}{\rho_b t_b}\right)}{\left(\frac{\bar{I}_b}{I_b} + \frac{E_p I_p}{E_b I_b}\right)}\omega_i^2\right)^{\frac{1}{4}} \tag{38}$$

where ω is free vibration natural frequency and C_i are constant coefficients that are computed by applying boundary conditions and the continuity conditions.

By applying a similar process to the process applied in section 4 one can write

$$eq_j = \frac{d^2 a_j(\tau)}{d\tau^2} + \sum_{i=1}^{M}\left[c\frac{da_i(\tau)}{d\tau}\int_0^1 \Phi_j^{norm}(x)\Phi_i^{norm}(x)dx \right] + a_j(\tau)\omega_j^2 + \alpha_3 P_{AC}\left(\left.\frac{dW_{2j}^{norm}}{dx}\right|_{l_1/l} - \left.\frac{dW_{3j}^{norm}}{dx}\right|_{l_2/l} \right) = 0 \tag{39}$$

where index *norm* denotes to the normalized mode shape. The unknown generalized coordinate $a_i(\tau)$ are obtained by solving the above ordinary differential equations. Same as previous section, static deflection and dynamic solution may be evaluated.

6. Result and discussion

Firstly, it is assumed that $\Omega = 0, P = P_{DC}$ i.e., the voltage is considered as DC. At this condition, the static deflection of clamped-clamped and cantilever microbeam are evaluated for three different positions and two thickness of piezoelectric layer. Then, the voltage is considered AC and these effects are studied by considering the mass inertia, excitation frequency and damping coefficient. The following geometric and mechanical properties which are the properties of Silicon and PZT5A are used (Wang *et al.* 2007). In addition the abbreviation described in Table 2 are used in order to concise the legend of figures.

Table 1 Geometrical and mechanical properties of considered microbeam

L (μm)	E_b (Pa)	E_p (Pa)	ρ_b (kgm^{-3})	ρ_p (kgm^{-3})	d_{31} (mvolt^{-1})	P_{DC} (volt)	P_{AC} (volt)
200	160× 10^{11}	67× 10^{11}	2300	7700	-1. 75× 10^{-10}	5	0.01

Table 2 Abbreviation used in the legend of figures

Abbreviation	Description
ASD1	Approximate static deflection using uniform microbeam mode shape as comparison function
ASD2	Approximate static deflection using non-uniform microbeam mode shape as comparison function
ESD	Exact static deflection
ADD	Approximate dynamic deflection using uniform microbeam mode shape as comparison function
EDD	Exact dynamic deflection given by modal expansion

6.1 Static deflection

The results for static deflection are shown in Figs. 2-8. Each figure includes a main part and two

adjoin parts. The adjoin diagrams shows that how the convergence occurs. The green adjoin diagram that is located at left side of figures, relates to the use of uniform microbeam mode shape and the blue diagram that is located at right side relates to the use of non-uniform microbeam mode shape as comparison function. The final converged responses and the exact solution has been plotted in main diagram.

It is observed from Fig. 2 that when a thin piezoelectric layer is deposited on the clamped-clamped microbeam from its clamped side to its middle part, then the Galerkin method converges to the exact solution using seven uniform microbeam mode shapes as comparison function. In addition, it shows that the convergence occurs with using three mode shapes of non-uniform microbeam as comparison function. It means that the required number of non-uniform microbeam mode shape for convergence is less than the required number of uniform microbeam mode shape.

If the geometry of system is symmetric it is expected that static deflection to be symmetric. Therefore, the symmetric mode shapes are only used as comparison function. In practice, the coefficients of asymmetric mode shapes are obtained about zero and will be negligible.

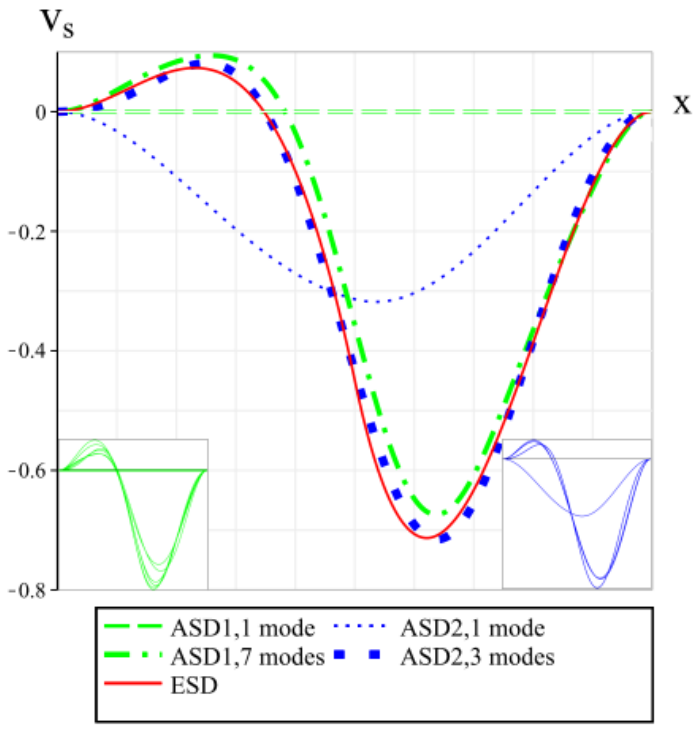

Fig. 2 The static deflection of clamped-clamped microbeam with $t_p = 0.5t_b$, $l_1 = 0$ and $l_2 = 0.5l$ calculated using three methods

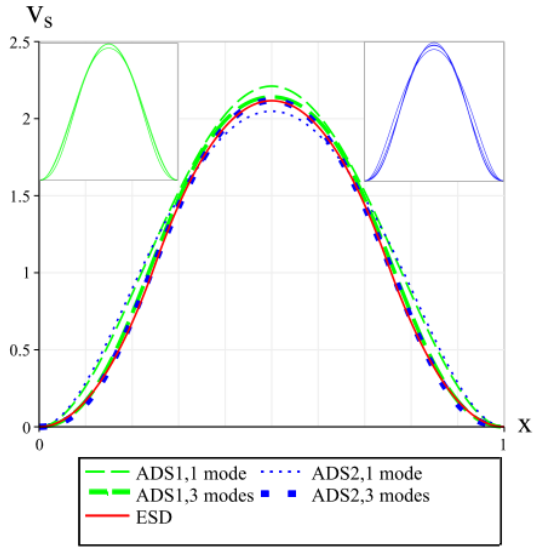

Fig. 3 The static deflection of clamped-clamped microbeam with $t_p = 0.5t_b$, $l_1 = 0.25$ and $l_2 = 0.75l$ calculated using three methods

So in Fig. 3 where the clamped-clamped microbeam is coated symmetrically by piezoelectric layer at its middle section, the symmetric mode shapes are used as comparison function. It shows that here which the thickness of piezoelectric layer is smaller than the thickness of based microbeam, $t_p = 0.5t_b$, there is not a main different between the use of uniform or non-uniform microbeam mode shape as comparison function. In addition, it shows that in this condition a good approximate solution is obtained using only one comparison function. It is noticeable that use of one mode made incorrect approximate solution in asymmetric geometry as shown in Fig. 2. It is observed from Fig. 4 that by increasing the thickness of piezoelectric layer from $t_p = 0.5t_b$ to $t_p = t_b$ the number of required uniform microbeam mode shape as comparison function for getting convergence is more than the number of required non-uniform microbeam mode shape.

Fig. 5 shows the static deflection of a cantilever microbeam which is coated by piezoelectric layer from left clamped side to the right. It is observed that the approximate solution using the first mode shape as comparison function is in excellent agreement with exact solution. It is observed in Fig. 6 that when the piezoelectric layer is deposited on the middle part of microbeam layer the number of required comparison function for getting convergence is two modes. Fig. 7 denotes that when the microbeam is covered by piezoelectric layer from free end side to the left, then the number of required comparison function for convergence has been increased to four modes. It can be concluded from Figs. 5-7 whenever the piezoelectric layer is closer to free end side, the number of modes that must be used increases. It is noted that here the thickness of piezoelectric layer is lower than the thickness of the based microbeam. It shows that there is not a main different between the use of uniform and non-uniform microbeam mode shape as comparison function. Fig. 8 demonstrates when the thickness of piezoelectric layer is more than the thickness of based microbeam, then the difference between the number of required uniform and non-uniform

comparison function for getting convergence increases.

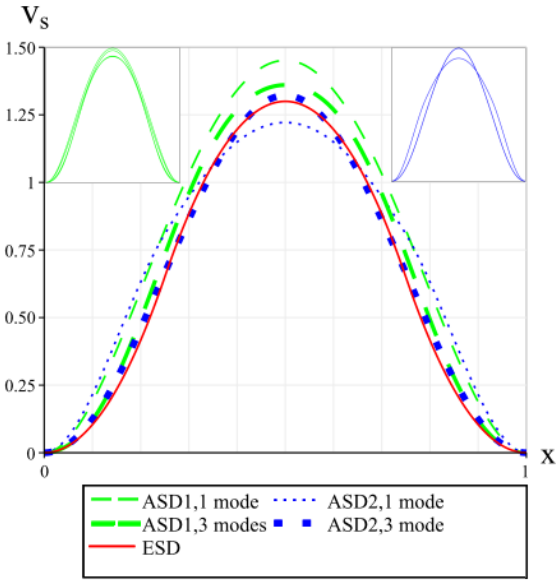

Fig. 3 The static deflection of clamped-clamped microbeam with $t_p = t_b$, $l_1 = 0.25$ and $l_2 = 0.75l$ calculated using three methods

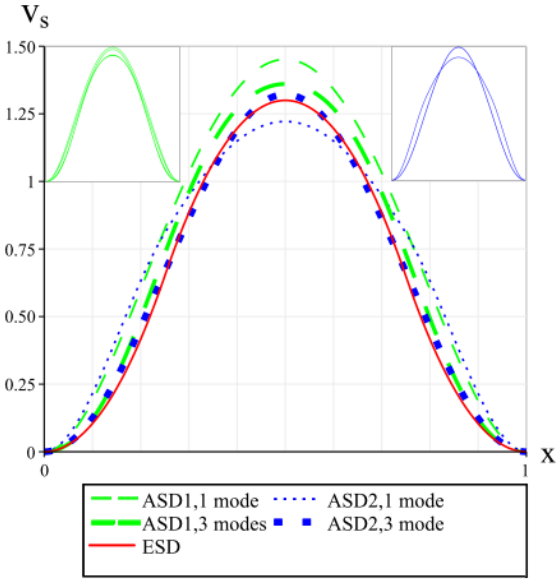

Fig. 4 The static deflection of clamped-clamped microbeam with $t_p = t_b$, $l_1 = 0.25$ and $l_2 = 0.75l$ calculated using three methods

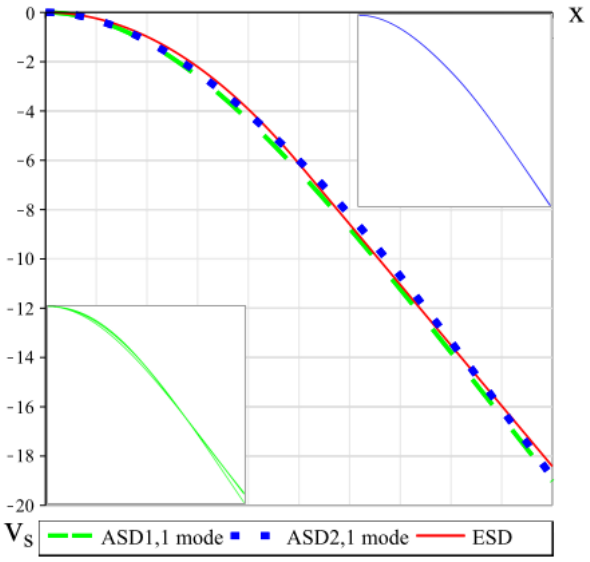

Fig. 5 The static deflection of cantilever microbeam with $t_p = 0.5t_b$, $l_1 = 0$ and $l_2 = 0.5l$ calculated using three methods

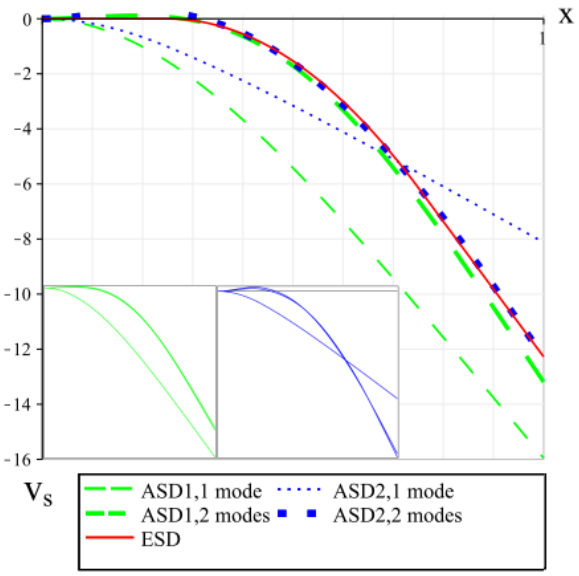

Fig. 6 The static deflection of cantilever microbeam with $t_p = 0.5t_b$, $l_1 = 0.25$ and $l_2 = 0.75l$.calculated using three methods

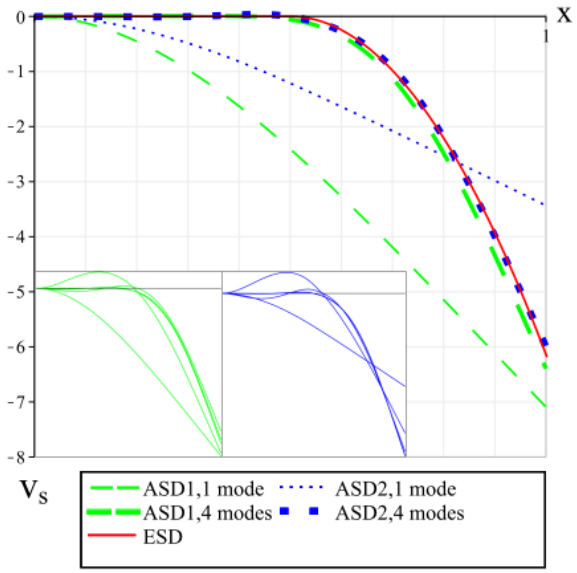

Fig. 7 The static deflection of cantilever microbeam with $t_p = 0.5t_b$, $l_1 = 0.5$ and $l_2 = l$ calculated using three methods

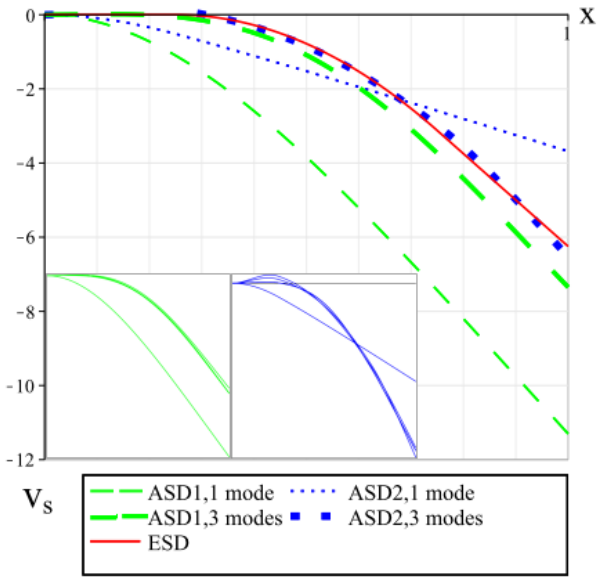

Fig. 8 The static deflection of cantilever microbeam with $t_p = t_b$, $l_1 = 0.25$ and $l_2 = 0.75l$ calculated using three methods

6.2 Dynamic deflection

Now, the results of dynamic solution is presented to determine the effects of comparison function, frequency of excitation, coefficient of external damping, location of piezoelectric layer, its thickness and length on the convergence. Firstly, the thickness of piezoelectric layer is considered $t_p = 0.5t_b$ i.e., lower than the thickness of based microbeam, and then it is decreased. Moreover, the coefficient of damping is assumed to be 0.02, and then it is increased to $c = 0.2$. The excitation frequency is considered approximately equal to the first natural frequency. It is noted that the time is considered to be large sufficiently in order to homogenous response to be damped completely. Fig. 9 shows the time history of the free end of microcantilever in which the piezoelectric layer is deposited on the entire length of based microbeam. It shows that there is a good agreement between the result of Galekin method and modal expansion solution. It is due to the fact that in this condition, the geometry of microbeam without piezoelectric layer and with piezoelectric layer is identical, and there is no change in the cross section of microbeam. It is shown in Figs. 10-13 that when the microbeam is covered by piezoelectric layer whose length is smaller than the length of based microbeam, then the difference between Galerkin method and modal expansion solution increases. Figs. 10 and 11 show that the time history at the free end side of microcantilever when the piezoelectric layer is deposited on the left part and middle part of based microbeam, respectively. In addition, Figs. 12 and 13 show the time history for the point of clamped-clamped microbeam whose amplitude deflection is maximum. In these figures, the piezoelectric layer is coated on the left part and middle part of the based microbeam.

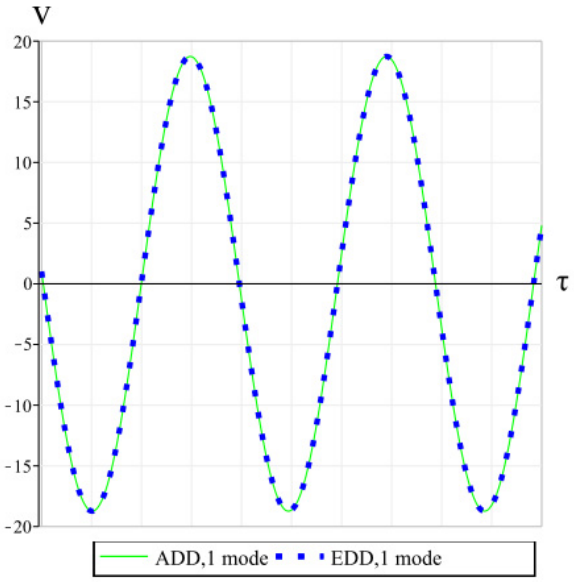

Fig. 9 The time history of cantilever microbeam with $t_p = 0.5t_b$, $l_1 = 0$, $l_2 = l$, $P_0 = 0.01volt$, $\Omega = \omega_1 = 3.2044$, $c = 0.02$ at $x = 1$ for τ from 2000 up to 2005

Figs. 9-13 denote that there is no difference between the given solution using one or two mode

shapes in the modal expansion solution when it is excited at the first natural frequency. It is noted that in the modal expansion theory the solution is expanded as a series of exact mode shape of structure. Here, the structure is excited near the resonance frequency, and the homogenous response is damped completely due to the viscous damping. So the corresponding excited mode contributes only in the response and the effects of other modes are negligible. It means that the modal expansion solution can be considered as an exact dynamic solution. Figs. 10-13 show that when the length of piezoelectric layer is smaller than the microbeam length, then there is a large difference between approximate solution given by Galerkin method and the solution given by modal expansion. These figures demonstrate that the Galerkin method solution dose not converge to the modal expansion solution even using five modes. It means that discretizing equation of motion using only the first mode shape of uniform microbeam as comparison function, which is usually applied in previous works, makes enormous error. It has been shown in the static solution that there is not main difference between the modal expansion solution and Galerkin method. It means that the induced difference in the dynamic solution is due to the excitation frequency, mass inertia and damping coefficient which is not appeared in differential equation governed to the static deflection.

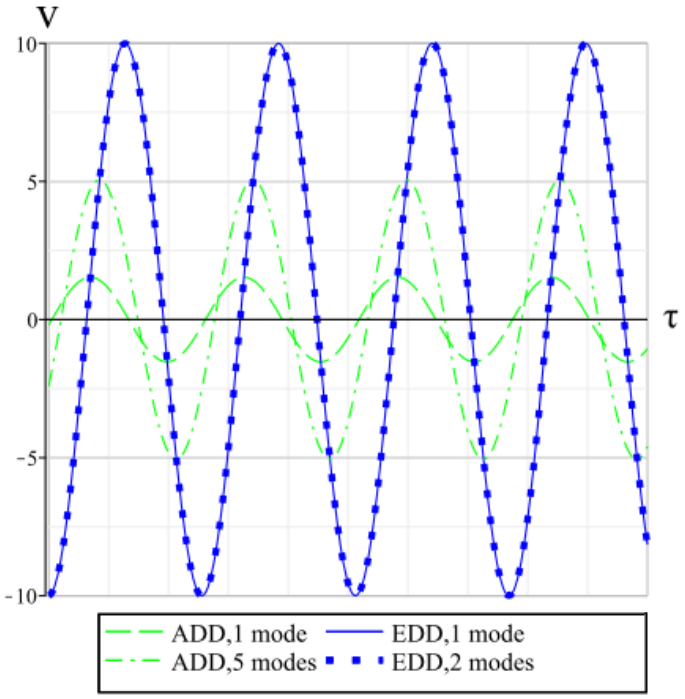

Fig. 10 The time history of cantilever microbeam with $t_p = 0.5t_b$, $l_1 = 0$ and $l_2 = 0.5l$, $P_0 = 0.01volt$, $\Omega = \omega_1 = 4.8985$, $c = 0.02$ at $x = 1$ for τ from 2000 up to 2005

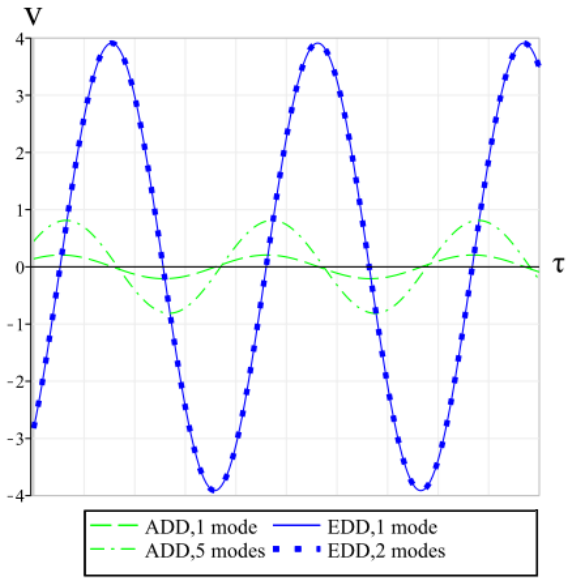

Fig. 11 The time history of cantilever microbeam with $t_p = 0.5t_b$, $l_1 = 0.25l$ and $l_2 = 0.75l$, $P_0 = 0.01volt$, $\Omega = \omega_1 = 3.0831$, $c = 0.02$ at $x = 1$ for τ from 2000 up to 2005

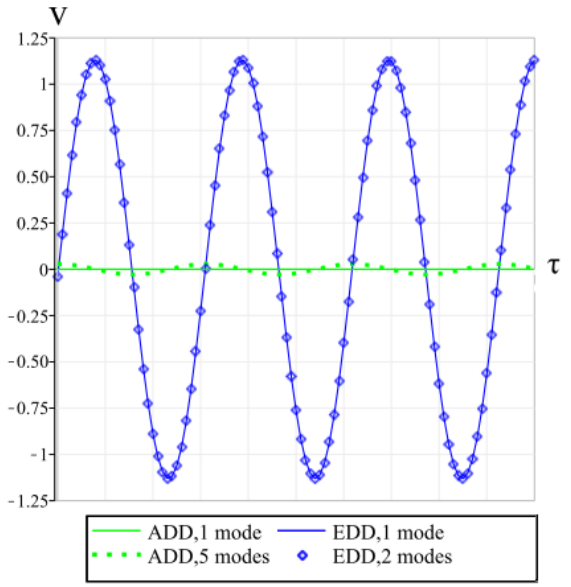

Fig. 12 The time history of clamped-clamped microbeam with $t_p = 0.5t_b$, $l_1 = 0$ and $l_2 = 0.5l$, $P_0 = 0.01volt$, $\Omega = \omega_1 = 20.4062$, $c = 0.02$ at $x = 0.5346$ for τ from 2000 up to 2001

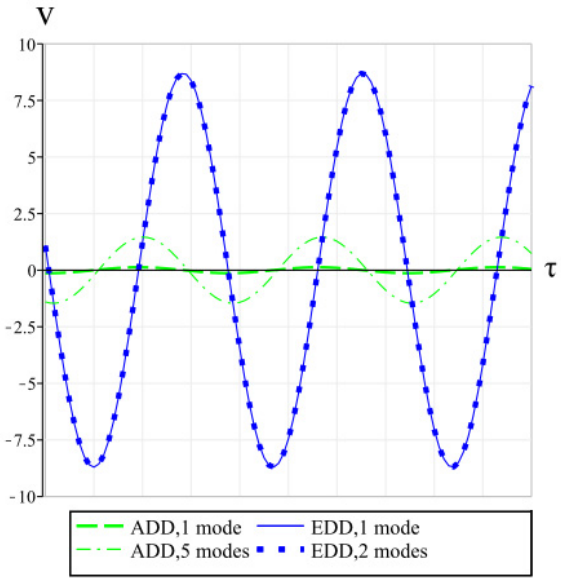

Fig. 13 The time history of clamped-clamped microbeam with $t_p = 0.5t_b$, $l_1 = 0.25l$ and $l_2 = 0.75l$, $P_0 = 0.01volt$, $\Omega = \omega_1 = 17.0415$, $c = 0.02$ at $x = 0.5$ for τ from 2000 up to 2001

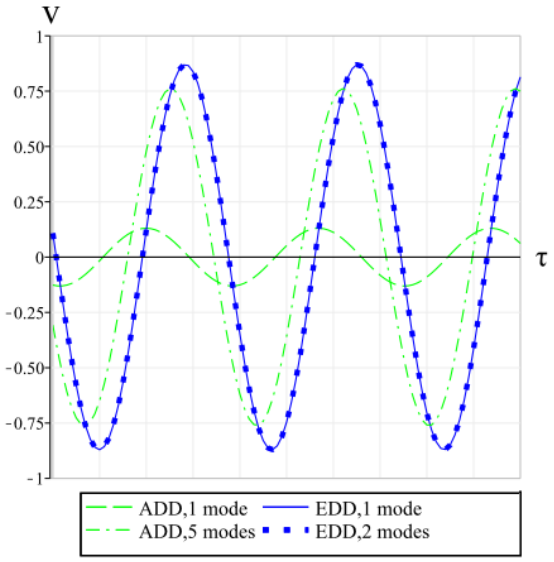

Fig. 14 The time history of clamped-clamped microbeam with $t_p = 0.5t_b$, $l_1 = 0.25l$ and $l_2 = 0.75l$, $P_0 = 0.01volt$, $\Omega = \omega_1 = 17.0415$, $c = 0.2$ at $x = 0.5$ for τ from 2000 up to 2001

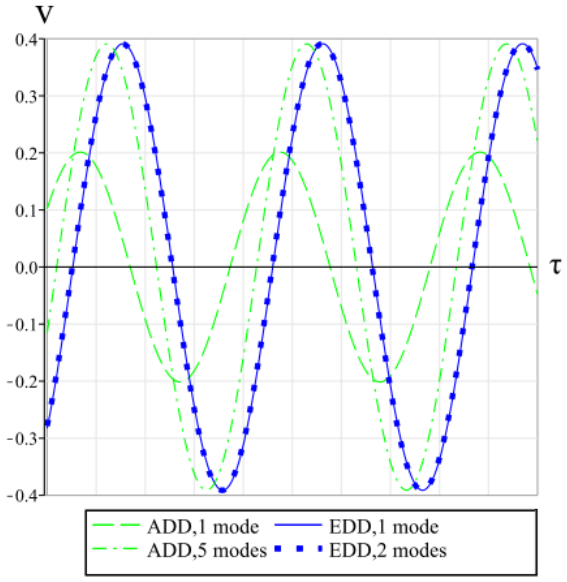

Fig. 15 The time history of cantilever microbeam with $t_p = 0.5t_b$, $l_1 = 0.25l$ and $l_2 = 0.75l$, $P_0 = 0.01volt$, $\Omega = \omega_1 = 3.0831$, $c = 0.2$ at $x = 1$ for τ from 2000 up to 2005

Now to investigate the effect of damping on convergence, coefficient of external damping is increased from 0.02 to 0.2. For brevity, one of above geometries, i.e., when the piezoelectric layer is deposited on the middle part of based microbeam is considered. According to Figs. 14 and 15, the convergence for both clamped-clamped and clamped-free microbeam is improved by increasing the coefficient of external damping. Although there is a good agreement between the modal expansion solution and Galerkin method solution but it occurs by using five mode shapes of uniform microbeam as comparison function. In other word, there is a considerable error when the equation of motion is discretized using only one mode shape as comparison function in the Galerkin method. Moreover in microresonators systems the coefficient of damping is to be considered very low.

These variations may be verified by considering the frequency response diagram i.e., FRF. Figs. 16 and 17 show the FRF diagram for clamped-clamped and cantilever microbeam. In these figures, the piezoelectric layer is coated on the middle part of based microbeam. It is noted that frequency associated to the peak point of amplitude response show the evaluated natural frequency. The convergence of fundamental natural frequency is shown in Table 3. In this table ω_1^n and ω_1^u are the first natural frequency calculated by using non-uniform and uniform comparison functions, respectively. According to the table when the piezoelectric layer is very thin or it covers the whole length of the microbeam, in other word when discontinuity in the microbeam cross section is diminished, the evaluated frequencies with both methods are the same. Whereas, when there is a discontinuity in the cross section, it is observed that the natural frequency obtained from approximate Galerkin method is few larger than the exact value, because the approximate method decreases the degree of system freedom. In this situation more modes are required in order to acquiring a good agreement between the evaluated natural frequencies in two methods of solution. Nevertheless of this agreement there is main difference between the time history solutions shown in Figs. 11-15. Considering Figs. 16 and 17, the amplitude of response given by Galerkin method may

be larger or smaller than the modal expansion solution. These variations may be confirmed by considering fig. 18. In this figure, a FRF diagram is shifted very small to the right or left with respect to the previous position. The amplitude of response at pick point of original FRF is called A, and corresponding frequency is called F_A . In addition the amplitude of response at point F_A on the shifted FRF is called B. It is clear that whatever the FRF is sharper, then the difference between A and B would be larger.

Figs. 16 and 17 show that the FRF diagrams given by modal expansion solution and Galerkin method are similar to original and shifted FRF considered in Fig. 18. Whenever the coefficient of damping is smaller, then FRF diagram would be sharper. It has been demonstrated in the upper paragraph that whatever FRF diagram is sharper then the difference between A and B would be larger. It means that by increasing the coefficient of damping, the difference between modal expansion solution and Galerkin method decreases.

Fig.18 denotes that the amplitude given from primitive and displaced FRF diagram is same if the detuning parameter and no the excitation frequency has been considered identical. It may be observed by comparing the amplitude at the points which is shown on the figure by A and C. It is noted that the purpose of detuning parameter is the distance of excitation frequency from the frequency of pick point at any diagram.

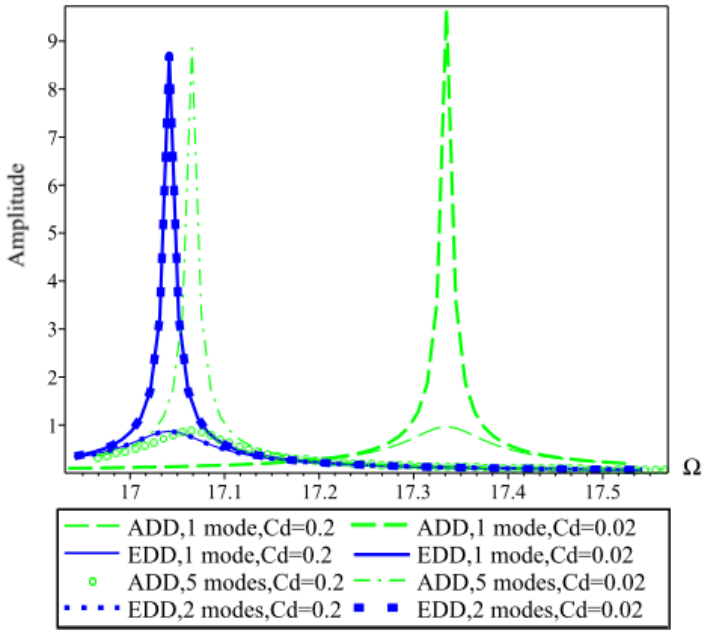

Fig. 16 The FRF of clamped-clamped microbeam for $x = 0.5$ with $t_p = 0.5t_b$, $l_1 = 0.25l$ and $l_2 = 0.75l$, $P_0 = 0.01volt$

Table 3 Natural frequencies

	Clamped-clamped microbeam	Cantilever microbeam

	$l_1 = 0.25l,\ l_2 = 0.75l,$ $t_p = 0.5t_b$		$l_1 = 0.25l,\ l_2 = 0.75l,$ $t_p = 0.001t_b$		$l_1 = 0.25l,\ l_2 = 0.75l,$ $t_p = 0.5t_b$		$l_1 = 0,\ l_2 = l,$ $t_p = 0.5t_b$	
	ω_l^n	ω_l^u	ω_l^n	ω_l^u	ω_l^n	ω_l^u	ω_l^n	ω_l^u
1	17.041506	17.334651	22.345230	22.345230	3.083069	3.352425	3.204397	3.204397
2	17.041506	17.106955	22.345230	22.345230	3.083069	3.155315	3.204397	3.204397
3	17.041506	17.083740	22.345230	22.345230	3.083069	3.121802	3.204397	3.204397
4	17.041506	17.075579	22.345230	22.345230	3.083069	3.121756	3.204397	3.204397
5	17.041506	17.065485	22.345230	22.345230	3.083069	3.117253	3.204397	3.204397

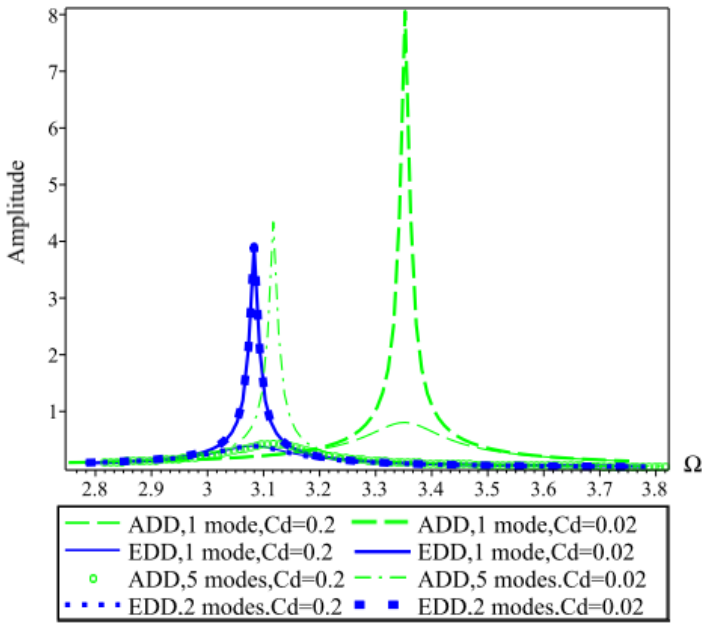

Fig. 17 The FRF of cantilever microbeam for $x = 1$ with $t_p = 0.5t_b$, $l_1 = 0.25l$ and $l_2 = 0.75l$, $P_0 = 0.01volt$

It has been mentioned in two previous paragraphs that the FRF diagrams given by modal expansion solution and Galerkin method are similar to the primitive and displaced FRF diagrams shown in Fig. 18. It means that when the detuning parameter is considered equal in Galerkin method and modal expansion solutions then the agreement between time histories may be better than when the excitation frequency is considered equal. In another word the excitation frequency in any method of solution must be considered equal to the adding of natural frequency evaluated in that method and

detuning parameter. It is noted that the approached method for inducing the agreement between the time histories given by modal expansion solution and Galerkin method is valid when the amplitude of pick point in FRF diagrams given by two methods of solutions be approximately same. It means that the coefficient numbers of comparison function must be used in Galerkin method. According to the previous results the number of required mode shape depends on the position and thickness of piezoelectric layer, damping coefficient and other parameters of systems. For example figure 16 shows that when damping coefficient is 0.02 then it is one mode, and Fig. 17 shows that it is five modes. It may be concluded that in many conditions if single uniform microbeam mode shape is used as comparison function of Galerkin method, then even if the detuning parameter be considered identical to the detuning parameter in modal expansion, then there is not a good agreement between the time histories of two methods of solutions.

Fig. 19 shows the time history of clamped-clamped microbeam coated by a thin piezoelectric layer i.e., $t_p = 0.001t_b$ at its middle section. It shows that in spite of that piezoelectric layer is deposited on a part of microbeam but there is a good agreement between modal expansion solution and Galerkin method. Comparing this figure and Fig. 13 shows that by increasing the thicknesses of piezoelectric layer the difference between Galerkin method and modal expansion increases.

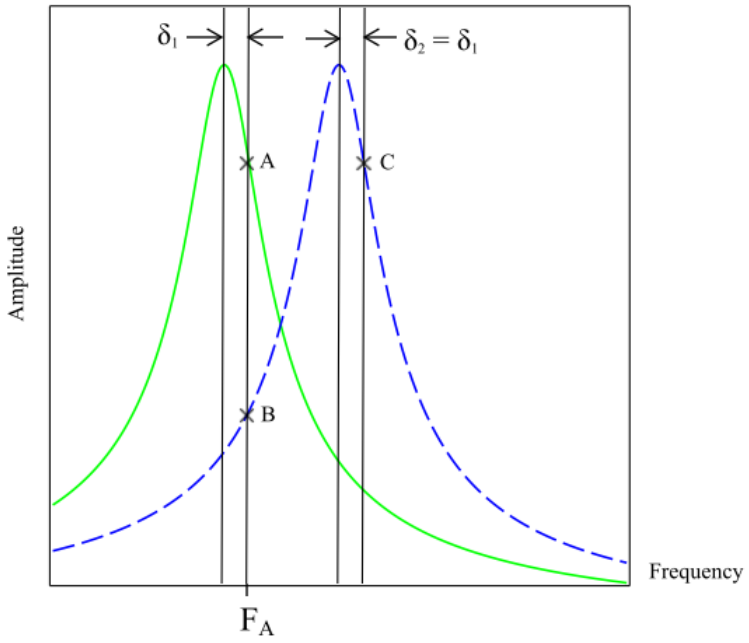

Fig. 18 An assumed FRF diagram, solid line belongs to the original diagram and dashed line belongs to the shifted diagram

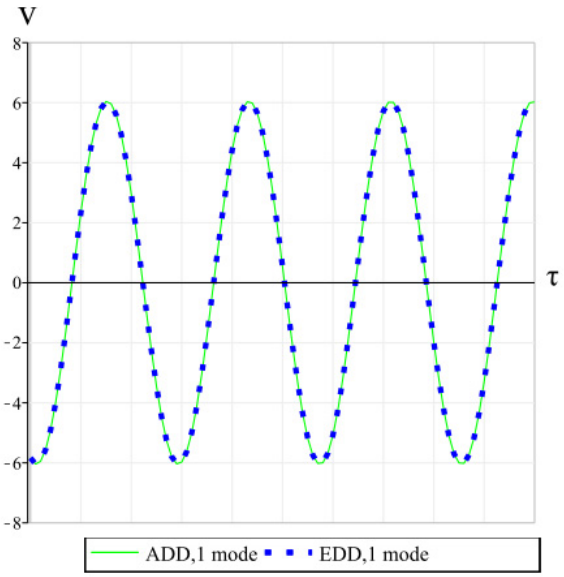

Fig. 19 The time history of clamped-clamped microbeam for $x = 0.5$ and τ from 2000 up to 2001 with $t_p = 0.001t_b$, $l_1 = 0.25l$ and $l_2 = 0.75l$, $P_0 = 0.01volt$, $\Omega = \omega_1 = 22.3452$, $c = 0.02$

Generally, the results showed that the error of solution due to the existing step changes in the cross section of microbeam is decreased by using the non-uniform microbeam mode shape as comparison function. Alternative method which can correctly model the cross section discontinuity is finite element method (Preidikman *et al*. 2007). In this method, a nod needs to be located exactly on the discontinuity point. Although, the finite element solution is straight forward but it yields to large computational process.

7. **Conclusions**

In this paper the Galerkin method is used for discretization, and a comprehensive analysis on the convergence of solution of equation that is discretized using uniform and non-uniform comparison function is studied for both clamped-clamped and clamped-free microbeams. The boundary conditions of microbeam have been considered as clamped-clamped and clamped-free. The static and dynamic solution resulted from Galerkin method has been compared to the modal expansion solution. In addition the static solution has been compared to the exact solution.

It is shown that the required number of uniform microbeam mode shapes for convergence of static solution depends on the position and thickness of deposited piezoelectric layer. The results demonstrated that when the based clamped-clamped microbeam is covered anti-symmetric by piezoelectric layer, then there is main difference between the required mode for convergence in modal expansion solution and Galerkin method. It has been shown that this result is confirmed for cantilever microbeam when it is coated from right free side to the left by a piezoelectric layer. It is observed that when the clamped-clamped microbeam is coated symmetrically by piezoelectric layer, then the convergence for static solution may be given using only first mode. This result is valid for

clamped –free when it is covered by piezoelectric layer from left clamped side to the right.

It is shown that there is a good agreement between the evaluated natural frequencies in modal expansion solution and approximate Galerkin method even using one comparison function. Nevertheless, the required number of uniform microbeam mode shape for convergence of time history due to AC actuation is much more than the required number of mode in modal expansion. This difference increases by increasing the piezoelectric thickness, the closeness of the excitation frequency to natural frequency and decreasing the damping coefficient. It has been observed that when the coefficient of damping is small, and the thickness of piezoelectric layer is multiple tenth of the based microbeam thickness, then the Galekin method does not converge even by using five numbers of comparison functions.

Considering the results of this paper one can conclude that using the uniform comparison function for discretizing the equation of motion of piezoelectrically actuated microresonator, results in an enormous error in response time history even for linear form. In practice the system under AC piezoelectric actuation has nonlinear behavior. When the convergence of linear system solution is given using high numbers of uniform modes, it is expected that the convergence of nonlinear system studied in previous works achieve by using more numbers of uniform comparison functions. But it is difficult to solve a nonlinear system including multiple discretized equations. So for decrease the response error of the previous work it is proposed that one non-uniform comparison function be used for discretization. It causes a decrease of the number of discretized equation and simplifying the procedure of solution.

References

Abramovich, H. (1998), "Deflection control of laminated composite beams with piezoceramic layers -closed form solutions", *Compos. Struct*., **43**(3), 217-231.

Azizi, S., Rezazadeh, G., Ghazavi, M. and Khadem, S.E. (2011), "Stabilizing the pull-in instability of an electro-statically actuated micro-beam using piezoelectric actuation", *Appl. Math. Model*., **35**(10), 4796-4815.

Azizi, S., Ghazavi, M., Khadem, S.E., Rezazadeh, G. and Cetinkaya, C. (2013), "Application of piezoelectric actuation to regularize the chaotic response of an electrostatically actuated micro-beam", *Nonlinear Dynam*., **73**(1-2), 853-867.

Bashash, S., Salehi-Khojin, A. and Jalili, N. (2008), "Forced Vibration Analysis of Flexible Euler-Bernoulli Beams with Geometrical Discontinuities", *Proceedings of the American Control Conference*, Washington, June.

Chen, C., Hu, H. and Dai, L. (2013), "Nonlinear behavior and characterization of a piezoelectric laminated microbeam system", *Commun Nonlinear Sci. Numer Simulat*., **18**(5), 1304-1315.

Dick, A.J., Balachandran, B., DeVoe, D.L. and Mote, J. (2006), "Parametric identification of piezoelectric microscale resonators", *J. Micromech. Microeng*., **16** (8), 1593-1601.

Ghazavi, M., Rezazadeh, G. and Azizi, S. (2010), "Pure parametric excitation of a micro cantilever beam actuated by piezoelectric layers, Microsyst Technol", *Appl. Math. Model*., **4** (12), 4196-4207.

Gopinathan, S., Varadan, V.V. and Varadan, V.K. (2000), "A review and critique of theories for piezoelectric laminates", *Smart Mater. Struct*., **9**(1), 24-48.

Hagedorn, P. and DasGupta, A. (2007), *Vibrations And Waves In Continuous Mechanical Systems*, John Wiley& Sons, Chichester, England.

Korayem, M.H. and Ghaderi, R. (2013), "Vibration response of a piezoelectrically actuated microcantilever subjected to tip–sample interaction", *Sci. Iran*., **20**(1), 195-206.

Li, H., Preidikman, S., Balachandran, B. and Mote, J. (2006), "Nonlinear free and forced oscillations of

piezoelectric microresonators", *J. Micromech. Microeng*., **16**(2), 356-367.
Li, H. and Balachandran, B. (2006), "Buckling and Free Oscillations of Composite Microresonators", *IEEE J. MEMS.*, **15**(1), 42-51.
Mahmoodi, S.N. and Jalili, N. (2007), "Non-linear vibrations and frequency response analysis of piezoelectricallydriven microcantilevers", *Int. J. Nonlinear Mech*., **42**(4), 577- 587.
Mahmoodi, S.N., Afshari, M. and Jalili, N. (2007), "Nonlinear vibrations of piezoelectric microcantilevers for biologically-induced surface stress sensing", *Commun Nonlinear Sci. Numer Simul*., **13**(9), 1964-1977.
Mahmoodi, S.N. and Jalili, N. (2008), "Coupled flexural-torsional nonlinear vibrations of piezoelectrically actuated microcantilevers with application to friction force microscopy", *J. Vib. Acoust*., **130** (6), 061003-1-10.
Mahmoodi, S.N., Jalili, N. and Ahmadian, M. (2010), "Subharmonics analysis of nonlinear flexural vibrations of piezoelectrically actuated microcantilevers", *Nonlinear Dynam*., **59**(3), 397-409.
Preidikman, S. and Balachandran, B. (2006), "Semi-analytical tool based on geometric nonlinearities for microresonator design" , *J. Micromech. Microeng*., **16**(3), 512-525.
Raeisi Fard, H., Nikkhah Bahrami, M. and Yousefi-Koma, A. (2014), "Mechanical characterization of electrostatically and piezoelectrically actuatedmicro-switches, including curveture and piezoelectric nonlinearities", *J. Mech. Sci. Technol*., **28**(1), 263-272.
Rezazadeh, G., Fathalilou, M. and Shabani, R. (2009), "Static and dynamic stabilities of a microbeam actuated by a piezoelectric voltage", *Microsyst. Technol*., **15**(12), 1785-1791.
Shooshtari, A., Hoseini, S.M., Mahmoodi, S.N. and Kalhori, H. (2012), "Analytical solution for nonlinear free vibrations of viscoelastic microcantilevers covered with a piezoelectric layer", *Smart Mater. Struct*., **21**(7), 075015 (10pp).
Simu, U. and Johansson, S. (2002), "Fabrication of monolithic piezoelectric drive units for a miniature robot", *J. Micromech. Microeng*., **12**(5), 582-89.
Wang, F., Tang, G.J. and Li, D.K. (2007), "Accurate modeling of a piezoelectric composite beam", *Smart Mater. Struct*., **16**(5), 1595-602.
Younis, M.I. (2011), *EMS Linear And Nonlinear Statics And Dynamics*, Springer, New York, USA .
Zamanian, M., Khadem, S.E. and Mahmoodi, S.N. (2008), "The effect of a piezoelectric layer on the mechanical behavior of an electrostatic actuated microbeam", *Smart Mater. Struct*., **17**(6), 065024 (15pp).

CC